Pulsating Flow Investigation for Spiked Blunt-Nose Body in Hypersonic Flow and its Control

Ashish Vashishtha[1,#]
Institute of Technology, Carlow, R93V960, Ireland

and

Shashank Khurana[2,#]
BITS Pilani, Dubai, 345055, United Arab Emirates

An aerospike, as a technique for drag reduction and heat transfer in high-speed flows, is associated with instabilities. To understand the pulsating flow behavior in front of forward facing spiked blunt nose, numerical investigation has been carried out using axisymmetric Navier-Stokes laminar flow solver at hypersonic Mach number 6.0. Initially flat, hemisphere and conical tip spiked blunt nose with flat-face cylindrical afterbody have been simulated for spike length-to-afterbody diameter ratio (*L*/*D*) of 2.0, with observing slight differences in the nature of pulsation. Furthermore, the pulsating flow field has been manipulated by introducing the corner radius (*r*) at the afterbody with variation of 0.1*D* and 0.2*D*. It is found that 0.2*D* corner radius can completely control the pulsation unsteadiness in front of different tip spiked blunt noses of *L*/*D* = 2.0.

I. Introduction

A forward-facing spike has largely and unanimously been identified and established as a passive flow control technique, to render the strong pressure envelope at the nose in high-speeds, to become weaker, thereby resulting in reduced pressure over the nose. As a consequence of vortices positioned at the spike root end, reduction in the heat transfer and drag is achieved. These key advantages, on the other hand, are challenged by the instability brought in the flow with the presence of a protruding surface. It produces an unbalanced normal component of force and the flow separation caused, and in turn oscillations, responsible for producing adverse moments along the surface of the body in consideration. In some cases, this could also have a negative effect on the drag reduction.

Previous researchers [1,2] have identified different types of unsteadiness in front of various spiked blunt noses in hypersonic flows. Further, Kenworthy [3] and Feszty et al. [4] have experimentally and

[#]Joint First Authors
[1] Assistant Lecturer, Department of Aerospace, Mechanical and Electronic Engineering, Institute of Technology, Carlow, Ireland. ashish.vashishtha@itcarlow.ie, AIAA Member.
[2] Assistant Professor, Department of Mechanical Engineering, BITS Pilani Dubai Campus, UAE, skhurana@dubai.bits-pilani.ac.in, AIAA Member.

numerically studied the driving mechanism of two distinct spike-induced unsteady flow modes as oscillation and pulsation. The oscillation flow mode is characterized by the foreshock shape change between a convex shape and a concave one, whereas the shock system changes dramatically in the pulsation flow mode. Further, Feszty et al. [5] have explained new mechanism of pulsations by numerical simulation method at Mach number 2.21 around a conical tipped spike with L/D = 1.0. Also, Feszty et al. [6] have confirmed about the mechanism of oscillatory mode fluctuations at supersonic and hypersonic Mach numbers for longer spike lengths. Balakalyani et al. [7] have recently found the pulsation (L/D = 0.7) and oscillatory flow (L/D = 1.8) for conical tip spike at hypersonic Mach number 6.0 in shock tunnel studies. Khurana et al. [8-9] conducted the flow visualization in a water channel for flat, conical, and hemispherical tip spikes at various Reynolds number and analyzed the effectiveness of different shapes analogically for hypersonic applications. Kalimuthu et al. [10] have studied, the effectiveness of conical, hemispherical, and flat tips of different spikes of length L/D = 0.5 to 2.0 for hemispherical-cylinder blunt nose and found the maximum drag reduction of 78 % for L/D = 2. However, no unsteadiness was reported with spiked body on hemispherical-cylinder blunt nose.

The pulsation unsteadiness has exhibited the features of higher amplitude and non-symmetry in the flow-field, which may lead to unsteady loads of high amplitude on forebody (spike face). The main motivation of the current study is to manipulate the flow field by slight modification in the geometry (passive flow control) to reduce the pulsation unsteadiness for spiked blunt nose in hypersonic flows. In the current study, numerical investigations have been performed with the following two objectives: (1) study the effect of spike tips: conical, hemispherical and flat spikes on flow unsteadiness for L/D = 2.0, and (2) controlling the flow pulsation by manipulating the shock interaction location on body corner by introducing the curvature.

II. Numerical Method

In the current study, two-dimensional structured grids have been generated in the computational domain for flat-face cylindrical base body with cylindrical spike. The computations are performed by solving unsteady axi-symmetric Navier-Stokes equations for laminar compressible flows. The spatial inviscid fluxes are evaluated by Lious all-speed AUSM (Advection Upstream Splitting Method) + up scheme [11] with upwind biased third order MUSCL (monotonic upstream-centered scheme for conservative laws) interpolation, while viscous fluxes as well as source terms (because of axi-symmetry) are evaluated by using second order central difference scheme. The third order TVD Runge-Kutta Method [12] was employed for time integration.

A. Computational Domain

In the current study, three different configurations of spikes with flat, hemispherical, and conical tips and same length of (L/D = 2.0) have been studied, initially for a flat-face of blunt nose body as shown in Fig. 1 (a) and (b). Here, L is the spike length and D is the maximum cross-sectional diameter of the base blunt nose (in current study, D = 40 mm). Further, to study the effects of afterbody corner shape, on pulsation of same spike configurations, the ratio of corner radius (r/D), have been changed for 0.1 and 0.2 until steady bow shock is achieved. The spike diameter (d) has been considered as d/D = 0.1 and for conical tip spike, cone angle has been used as θ = 30°. Figure 1(c) shows the structured grid generated using elliptic grid

generation method for conical tip spike and corner radius of blunt nose r/D = 0.1. For all the cases, the domain is used with 151x101 grid points after grid independence test.

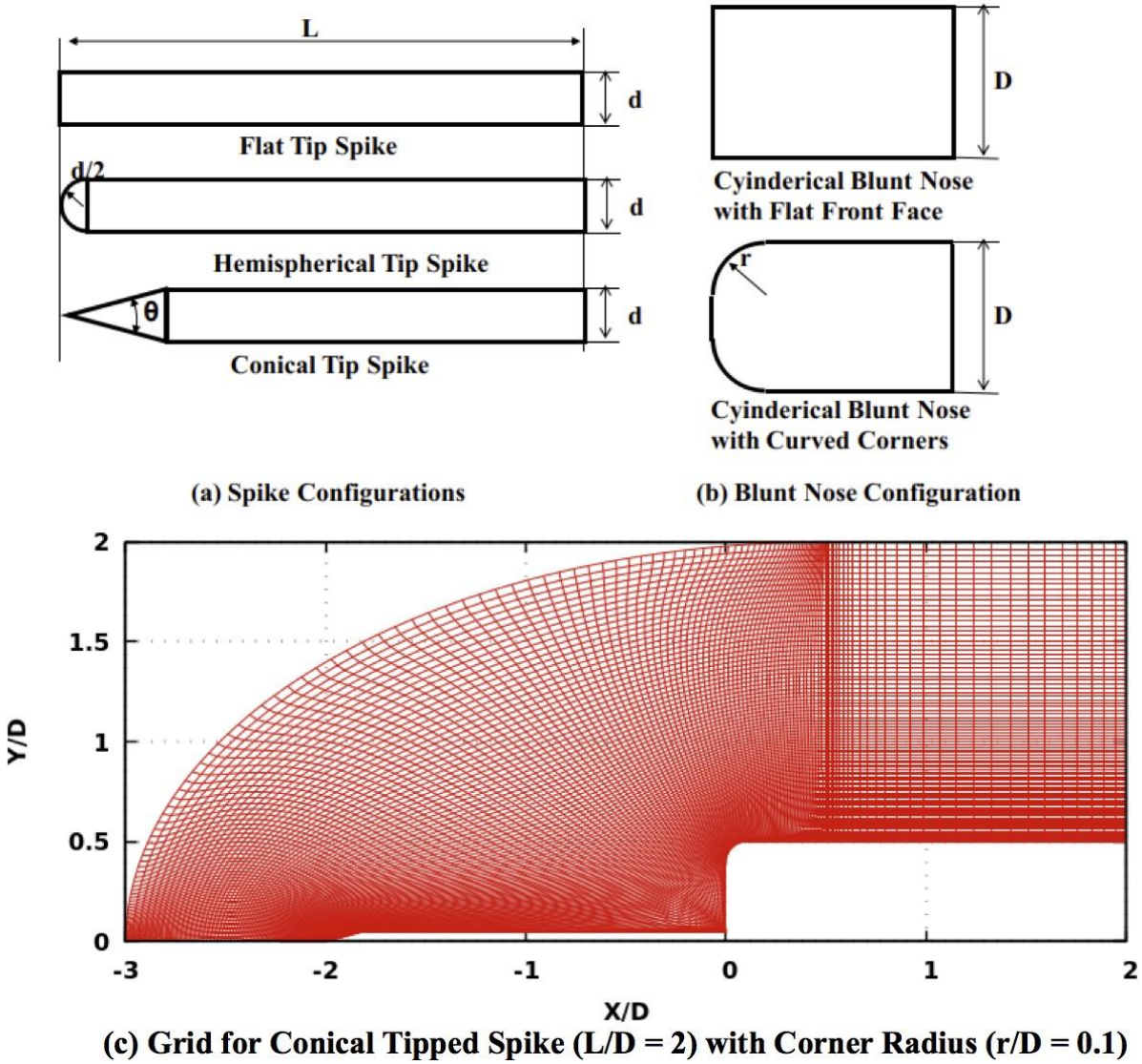

Fig. 1. (a) Configurations of Spikes, (b) Configuration of afterbody, (c) Grid generated for conical spike and curved corner case.

B. Boundary and Initial Conditions

The boundary condition at the inlet section is considered according to the flow condition used by Feszty et al. [4] of hypersonic flow Mach 6.0. However, the reference length or diameter of blunt nose have been used as 40 mm for current study as shown in Table 1. At the wall, no-slip boundary condition, along with isothermal constant wall temperature 300 K, is assumed. The outlet is treated as supersonic outlet with first order interpolation of fluxes from the inner domain. The flow is initiated with low velocity around the spike and blunt nose and is considered to have an impulse start. All the computations have been performed for a duration of 4 ms.

Table 1. Inlet Boundary Conditions

Parameter	Values
Mach Number (M)	6.0
Reference Length (D)	40 mm
Stagnation Pressure (P_0)	400 kPa
Adiabatic Wall Temperature (T_w)	300 K
Reynolds Number (R_e)	0.134×10^6

C. Code Validation / Grid Independence

In order to evaluate performance of the current code, the simulation are performed for conical tipped spike for flat-face cylindrical blunt nose, similar to Feszty et al. [4] for hypersonic flow condition, where the reference diameter (*D*) is 46 mm and spike diameter *d*=0.065*D*. The computation grids are generated with maximum dimensions of 4mm, 2mm and 1 mm as coarse (76 x 51), medium (151 x 101) and fine (301 x 201) grid, respectively. The computations are performed for Mach Number 6.0 and Reynolds number of 0.134 million. Figure 2 shows the results obtained from the simulations for 4 ms time-interval for all three grid configurations. Figure 2(a) shows the non-dimensional pressure ($P/\rho V^2$) variation at *Y*-location of *D*/2 on the front face and Fig. 2(b) shows the variation of drag coefficient with time. The various phases of pulsating flow cycle (collapse, withhold and inflate) have been observed for all three grid configurations. During the initial cycles of pulsating flow, it can be seen that for all three grid sizes, the pressure and drag coefficients have been behaving in a similar manner, while after 2 ms, there is a slight phase difference between pulsation cycles. However, variation in pressure and drag coefficients have almost similar amplitude, with very small phase differences for medium and fine grids. Hence, 2 mm medium grid size have been used in all the further studies. The non-dimensional Strouhal Number, which is defined as $\left(S_R = \frac{fD}{V_\infty}\right)$, have been found as 0.114 after 2 ms, and non-dimensional pressure fluctuations have been in the range of 0 to 2 for 2mm grid case, which can be considered close to Feszty [4] results and the accuracy of current simulations methods can be considered adequate for the current comparative study.

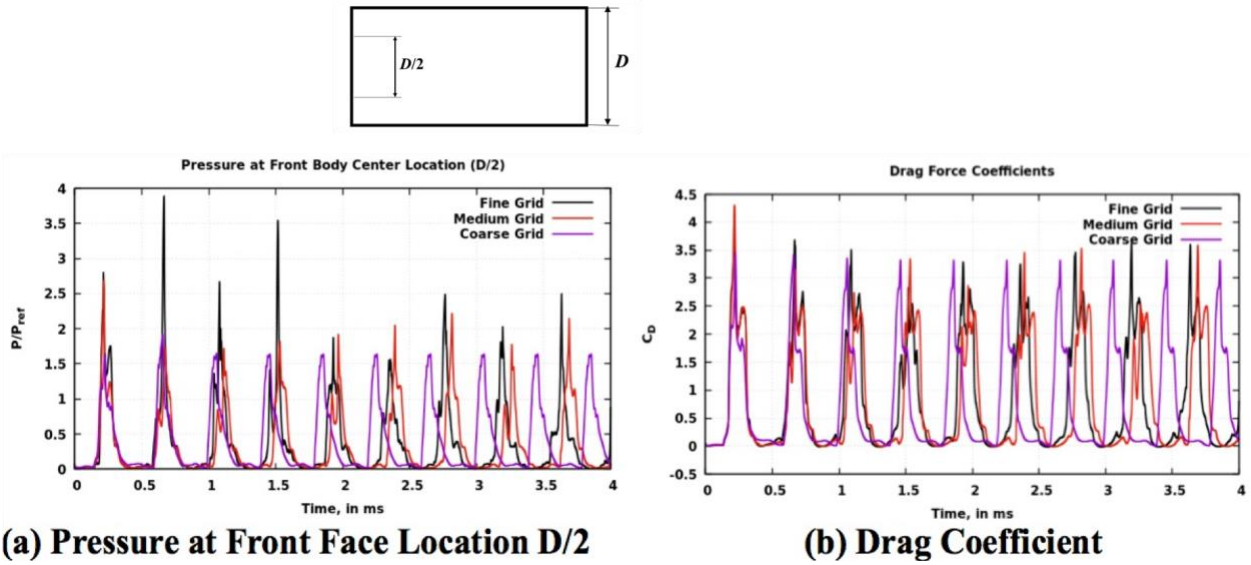

Fig. 2. (a) Pressure at front face, and (b) Drag Coefficient variation with time for different grids.

III. Results and Discussions

The further computations have been performed for reference diameter, D = 40 mm, and spike diameter d/D = 0.1 and spike length L/D = 2.0. The freestream conditions are also same for all the studies as Mach number 6 and Reynolds Number 0.134 million. Initial study has been performed to study the effect of spike tip with flat, hemispherical, and conical nose shapes in front of flat-face cylindrical afterbody. Further, investigation has also been conducted by a curvature of radius r/D = 0.1 and 0.2 on the afterbody nose, with a strong evidence of reduction of pulsations in the flow field.

A. Effect of Spike Tips

The numerical simulations have been performed for three spike tips: conical, hemispherical, and flat. According to Feszty et al. [5], in supersonic flows, the pulsation mechanism consists of three processes: collapse, inflation and withhold. Figure 3(a) and 3(b) shows Mach number contours for the end of inflation and collapse phases, respectively for flat, hemispherical, and conical spike tips. In case of flat and hemispherical tip noses, vertical normal shock exists in front of spiked body, while in case of conical tipped spike blunt nose, the standing shock is slightly curved. At the end of collapse phase, the triple point of forebody and afterbody shocks is closer to the front face of blunt nose in case of conical tip spiked body, while it is slightly away in other cases, which leads to higher maximum pressure in conical tip case in Fig. 4(a). Figure 4(a) shows the non-dimensional pressure fluctuation at $D/2$-location on flat-face of cylindrical blunt nose and Fig. 4(b) shows the variation of drag coefficient on the body. As the main source of unsteadiness is pulsation mechanism in this case, the variation in pressure location and drag coefficient have similar trend for hemispherical and flat spike tips, while for conical spike tip there is phase difference in both the plots of pressure at $D/2$-location and drag coefficients. Within 4 ms, for hemispherical and flat spike tips, the number of cycles of pulsation have been observed to be 11, while for conical spike tip they stood at 10. The time-averaged frequency, and corresponding Strouhal number of repeating pulsations, are 2500 Hz, 0.106 for conical spike tip and 2750 Hz, 0.117 for hemispherical and flat spike tip respectively. The main reason for this difference is attributed to the spike nose shapes, with flat and hemispherical tips of spike leading to the formation of a bow shock in front of it, with conical tip spike generating an oblique shock.

For the current study, the mechanism of pulsation can be described from the non-dimensional pressure plot in Fig. 4(a). As the pressure reaches minimum, the inflation process has almost ended, and the spike is likely immersed in the subsonic flow behind the standing normal shock. The withhold phase in the current cases is momentarily, probably because of high momentum in hypersonic flows. The rise in the pressure at the front face is caused by end of the collapse process when the foreshock and after shock interaction point comes closer to the bunt nose front face.

From these simulations, it is understood that after the end of collapse phase, the following inflation phase is caused by a sharp corner at the flat-face of afterbody, which requires a slight build up in pressure for the escape of the mass accumulated in the zone between spike root and afterbody front face. A small pressure gradient near the afterbody corner may reduce the shock unsteadiness. Therefore, the numerical simulations are performed by introducing a curvature at the corner with radius r at the afterbody front face, by varying r/D = 0.1 and 0.2 until pulsation fluctuations are reduced.

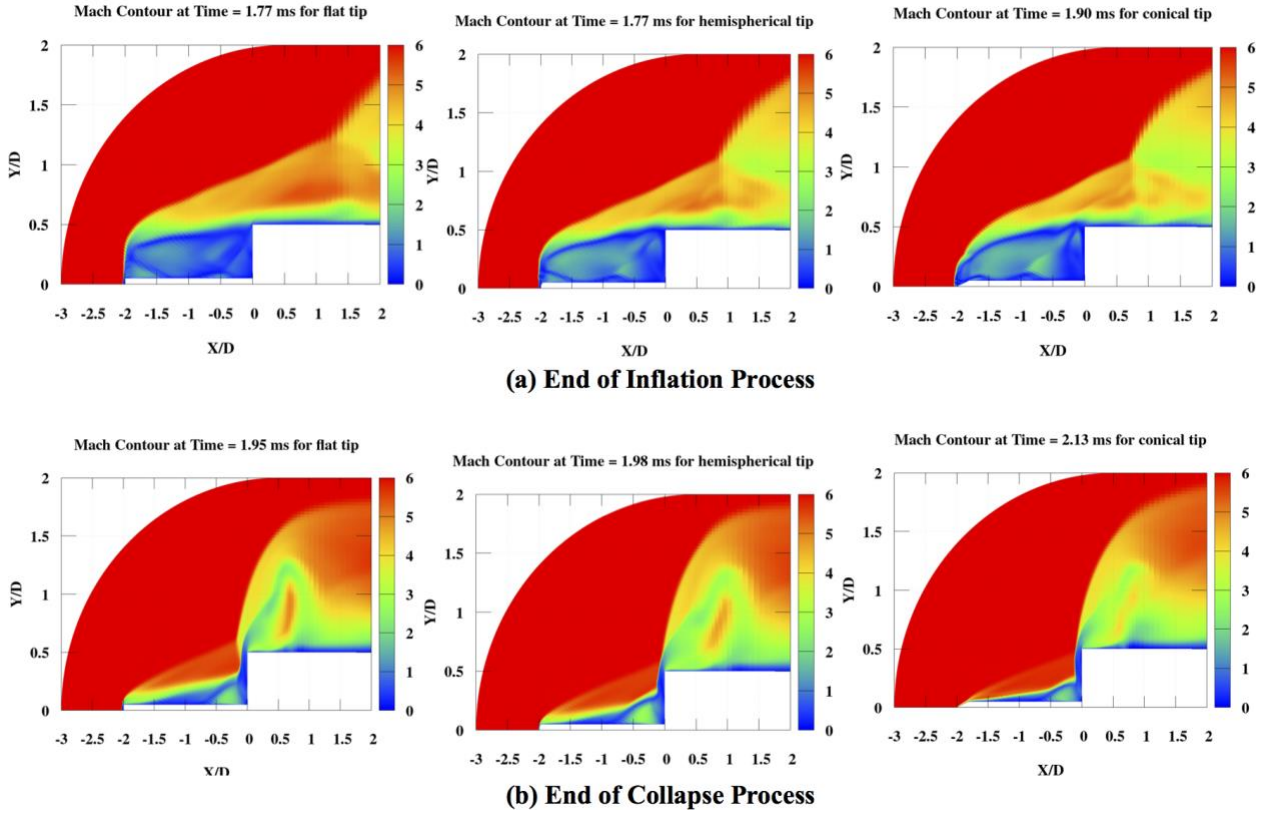

Fig. 3. Mach Number Contours for different phases in pulsation unsteadiness for Different Spike Tips in front of a Flat-Face afterbody.

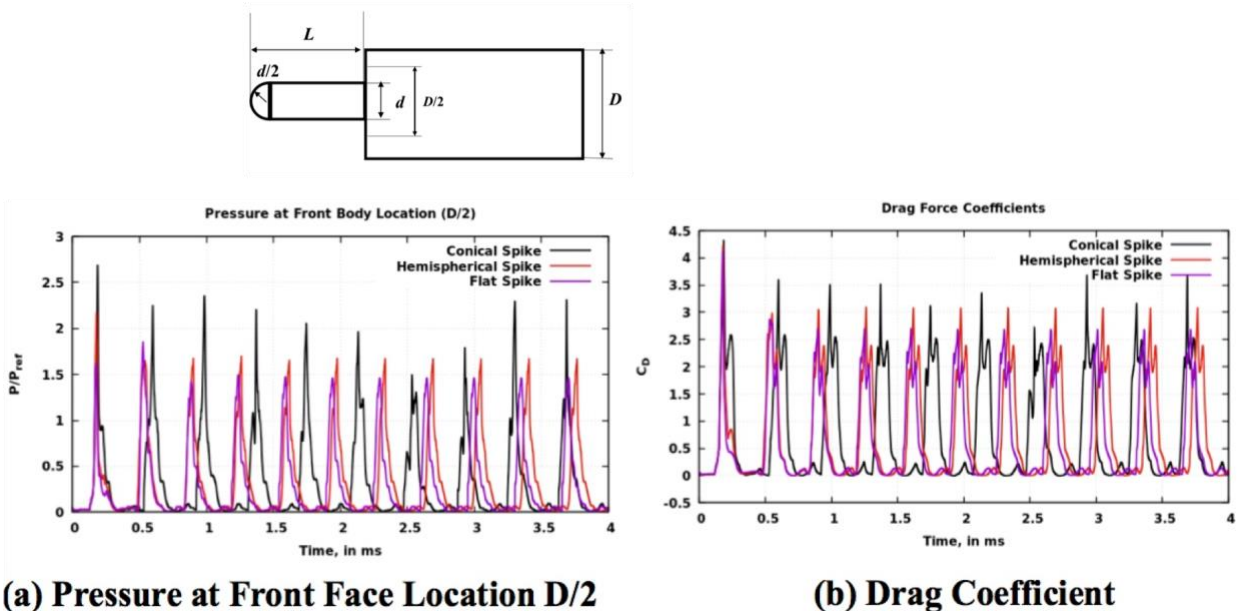

Fig. 4. (a) Pressure at front face and (b) Drag Coefficient variation with time for Different Spike Tips with Length L/D = 2.

B. Flow Control by Corner Curvature

The sharp corner in case of flat afterbody blunt nose, with L/D = 2.0 spike, contributes to pulsation unsteadiness as foreshock and aftershock can interact near it. Hence, by introducing a curvature at the corner, it is attempted to move the interaction point away from the body. In this section, the results from simulation of spike with flat, hemisphere and conical tips have been discussed for corner radius on cylindrical blunt nose of afterbody for r/D = 0.1 and 0.2. Figure 5 represent the Mach number contours for different spike nose cases with the variation in the corner radius of afterbody. Figure 6(a) shows the non-dimensional pressure variation at $D/2$ location and over all drag coefficient variation for corner radius r/D = 0.1, while Fig. 6(b) shows the same plots for corner radius r/D = 0.2.

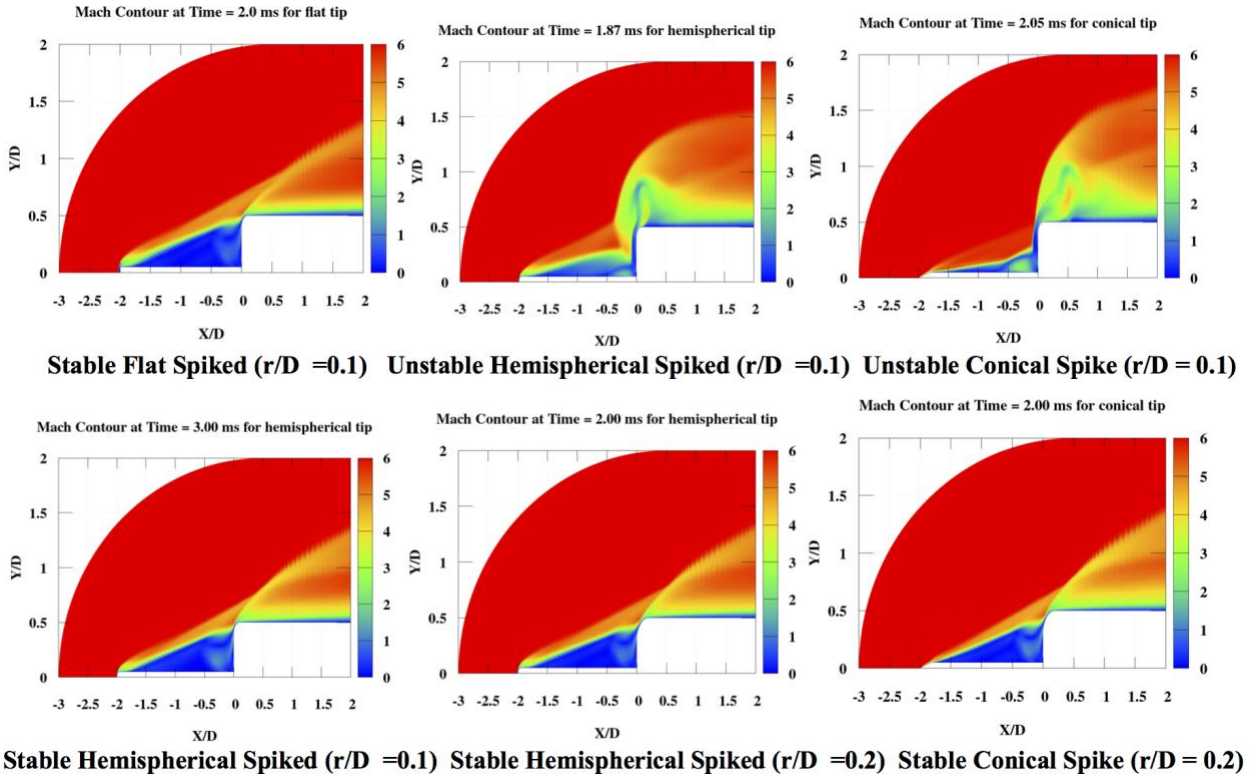

Fig. 5. Different Stable and Unstable (End of Collapse Phase) Flow Field Configuration for different spike tipped blunt nose with corner radius, r/D = 0.1 and 0.2

Figure 5 shows different stable and unstable flow field Mach number contours for hemispherical and conical tip spiked blunt nose with corner radius of front face varying r/D= 0.1 and 0.2. Figure 5 (top left) shows the steady field for flat tip spike afterbody with a corner radius of 0.1D. It can be observed that the forebody (spike bow shock interacts with afterbody bow shock far from the corner in Edney Type V interaction [13], and the shear layer stabilizes near the corner. In case of hemispherical tip spike, with afterbody corner radius of 0.1D, initially pulsations are observed, as seen in Fig. 5 (top-middle) at the time instant of 1.87 ms, which corresponds to the end of collapse phase of pulsation. It can be seen that the forebody shock interacts with afterbody shock before the flat-face of afterbody, and corner might not be initially provide enough relaxation, while at time 3 ms (bottom left figure) forebody shock stabilize itself and does not show unsteady pulsation. In case of conical tip spiked blunt nose with corner radius 0.1D, the pulsations are

prominently visible from Fig. 6(a), while Fig. 5 (top right) shows the Mach number contours at the end of collapse phase. Further, corner radius is varied to 0.2*D* for hemispherical and conical tip spike cases, and both the cases shows stable flow field, as illustrated in Fig. 5, (bottom middle for hemispherical tipped, and bottom right for conical tipped spike). The difference in behavior for unsteady and steady flows around different tip spiked blunt nose is because of the difference in forebody shock and its inclination for different afterbody noses. A strong bow shock formed in front of flat tipped spike with bigger envelop, while hemispherical tipped spike has forebody shock as bow shock with slightly lesser inclination than the flat tipped spike. The conical tip spiked blunt nose have oblique shock with the least inclination and can interact with the front face of afterbody at the least height of the face. Hence, the corner radius *r/D* = 0.1 is sufficient to reduce the pulsation for flat tipped spike, while a corner radius 0.2*D* is required for a completely stable flow for hemispherical and conical tipped spike cases. It can be said that the forebody shock interaction point on the front face of afterbody determines the corner radius requirement. The forebody shock inclination changes from higher to lower for flat, hemispherical, and conical tips in sequence. The required corner radius for flat tipped spike is *r/D* = 0.1 and for hemispherical and conical tipped spike the required corner radius is *r/D* = 0.2. It is interesting to see that *r/D* = 0.1 shows both pulsation and stable flow behavior for hemisphere tipped spiked body.

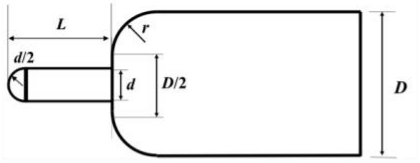

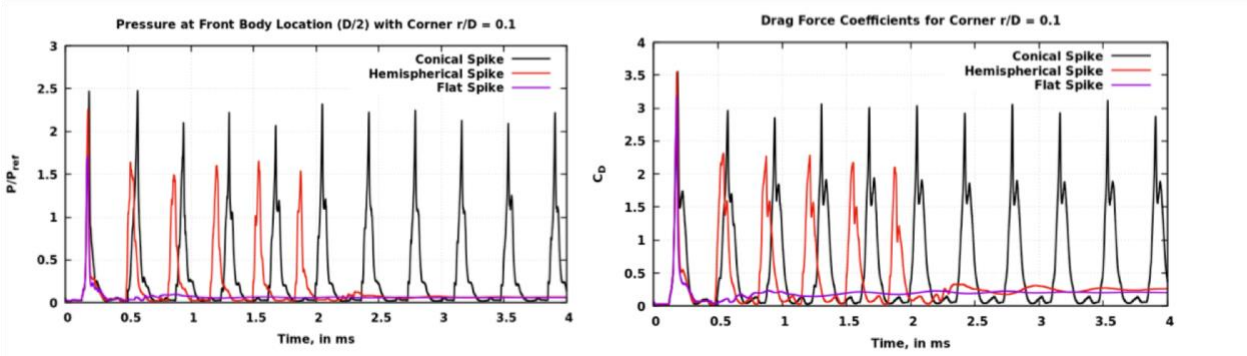

(a) Pressure at Front Face Location D/2 (left) and Drag Coefficient (right) for r/D = 0.1

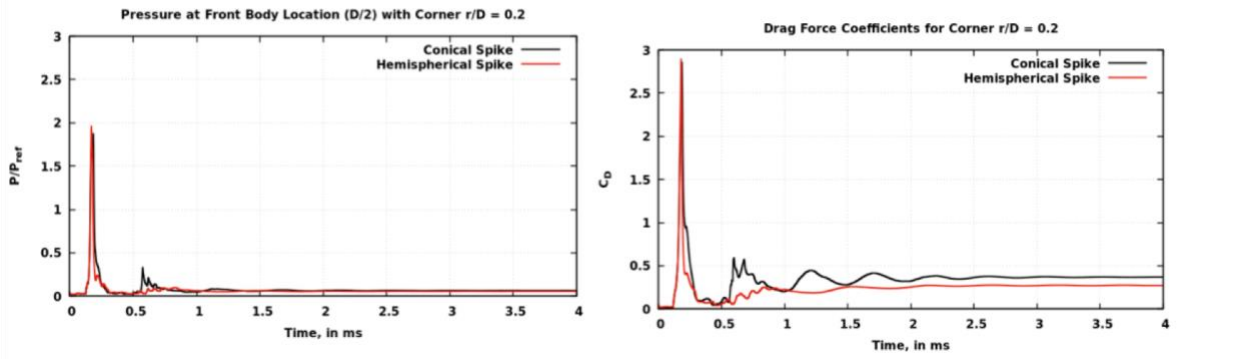

(b) Pressure at Front Face Location D/2 (left) and Drag Coefficient (right) for r/D = 0.2

Fig. 6. Non-dimensional Pressure and Drag Coefficient variation for different tipped spike and corner radius *r/D* = 0.1, 0.2

It can be inferred from Fig. 6(a) that the unsteadiness of pulsation is completely removed by introducing a corner radius of r/D = 0.1 for flat tipped spiked body. A hemispherical tipped spike, with a corner radius r/D =0.1, initially shows pulsations but the pulsations gets completely transitioned to stable flow behavior after 2 ms. For conical tipped spiked body, the pulsation continues even for corner radius r/D = 0.1, but with even smaller withhold time. As a result of this, only hemispherical and conical tipped spikes are simulated with a corner radius r/D = 0.2. Figure 6(b) shows that after an initial hike in the non-dimensional pressure and drag coefficients, owing to an impulse start, the pulsations are completely subsided for both the cases. However, there is a slight unsteadiness in the conical spike case, but it also becomes stable in the later part of the time domain after 2.5 ms. In stable flows, the drag coefficient (in Fig. 6) for flat tip spike is estimated as 0.21, while for hemispherical and conical tip cases, it is 0.27 and 0.37 respectively. These results are almost same for L/D=2.0 cases experimentally studied by Kalimuthu et al. [10] at Mach 6.0 for hemisphere-cylinder blunt nose afterbody with different spike tips. In future studies, it will be of great interest to understand the mechanism of stabilizing the pulsation or transition between pulsation and oscillation for different size of spiked blunt noses.

IV. Conclusions

In the current study, the unsteady behavior of flow field in front of flat, hemisphere and conical tip spikes with length L/D = 2.0, with blunt nose (flat-face and with corner radii) afterbody have been investigated using axisymmetric numerical simulations. It is found that forebody shock of different tipped spike interacts with afterbody shock in different manners and leads to slightly different pulsation frequencies. Further introduction of curvature at the corner of flat face afterbody lead to control the pulsation effectively. A flat tipped spike with 0.1D corner radius leads to stable flow immediately, while hemisphere tip spike nose with corner radius 0.1D shows initially pulsation behavior and after few cycles becomes stable, and the conical tip spike with corner radius 0.1D shows pulsation behavior during the simulation duration. For hemisphere and conical tip spikes, with afterbody corner radius of 0.2D, a stable flow behavior is witnessed with complete control of pulsation. The calculated drag coefficients for stable flows in front of flat, hemispherical, and conical tip spiked bodies, with corner radius of 0.2D, registers approximate similar values for hemispherical cylinder afterbody with same spike configurations.

References

[1] Maull, D. J., "Hypersonic flow over axially symmetric spiked bodies", *Jl. Fluid Mechanics*, Vol. 8, No. 4, 1960, pp. 584-592.

[2] Wood, C.J., "Hypersonic Flow Over Spiked Cones," *Jl. Fluid Mechanics*, Vol. 12, Part 4, 1961, pp. 614-624.

[3] Kenworthy, M.A, "A Study of Unstable Axisymmetric Separation in High Speed Flows", PhD Thesis, Virginia Polytechnic Institute, 1978.

[4] Feszty, D., Badcock, K.J., Richards, B.E., Woodgate, M.A., "Numerical simulation of a pulsating flow arising over an axisymmetric spiked blunt body at Mach 2.21 and Mach 6.00", *Shock Waves*, Vol. 10, No. 5, 2000, pp. 323-331.

[5] Feszty, D., Badcock, K.J., Richards, B.E., "Driving mechanisms of high-speed unsteady spiked body flows. Part 1", *AIAA Jl.*, Vol. 42, No. 1, 2004, pp. 95-106.

[6] Feszty, D., Badcock, K.J., Richards, B.E. "Driving mechanisms of high-speed unsteady spiked body flows. Part 2", *AIAA Jl.*, Vol. 42, No. 1, 2004, pp. 107-113.

[7] Balakalyani, G., Sriram, R., Jagadeesh G., "Shock Tunnel Studies of the Unsteady Hypersonic Flowfield Around Spiked Bodies", *Proceedings of 30th International Symposium on Shock Waves-2*, 2017, 74, pp. 1217-1222.

[8] Khurana, S., Suzuki, K., Rathakrishnan, E., "Flow field behavior with Reynolds number variance around a Blunted-nosed Body with Spike", *Modern Physics Letters B*, 30, 2016, 1650362, pp. 1-13.

[9] Khurana, S., Suzuki, K., Rathakrishnan, E., "Visualization of Vortex at Aerospike Root using Hydraulic Analogy", *International Review Aerosp. Engg. Jl.*, Vol. 10, No. 4, 2017, Page 189-195.
[10] Kalimuthu, R., Mehta, R.C., Rathakrishnan, E., "Investigation of aerodynamic coefficients at Mach 6 over conical, hemispherical and flat-face spiked body", *The Aeronaut. Jl.*, Vol. 121, No. 1245, 2017, pp.1711-1732.
[11] Liou, M.S., "A sequel to AUSM, Part II: AUSM$^+$-up for all speeds", *Jl. of Comp. Physics*, Vol. 214, No. 1, 2006, pp. 137-170.
[12] Shu, C.W., Osher S., "Efficient implementation of essentially non-oscillatory shock-capturing schemes", *Jl. of Comp. Physics*, Vol. 77, No. 2, 1988, pp. 439-471.
[13] Edney, B.E., "Effects of Shock Impingement on the Heat Transfer around Blunt Bodies", *AIAA Jl.*, Vol. 6, No. 1, 1968, pp. 15-21.